



# Flexible 3D carbon nanotubes cuff electrodes as a peripheral nerve interface

Pan Tian<sup>1</sup> · Wenwen Yi<sup>2</sup> · Chaoyang Chen<sup>3</sup> · Jie Hu<sup>1</sup> · Jin Qi<sup>1</sup> · Boshen Zhang<sup>2</sup> · Mark Ming-Cheng Cheng<sup>2,3</sup>

Published online: 19 February 2018  
© Springer Science+Business Media, LLC, part of Springer Nature 2018

## Abstract

The cuff electrode provides a stable interface with peripheral nerves, which has been widely used in basic research and clinical practice. Currently, the cuff electrodes are limited by the planar processing of microfabrication. This paper presents a novel cuff electrode using high-aspect ratio carbon nanotubes (CNTs) integrated on a flexible biocompatible parylene. The microfabrication process unites the high quality vertical CNTs grown at high temperature with the heat sensitive parylene substrate in a highly controllable manner. The fabricated cuff electrodes have been utilized for extracellular nerve stimulation in rats. The experimental results demonstrate the proposed CNT electrode has a better performance than Pt electrode in nerve stimulation. Moreover, the effect of electrode position and stimulation frequency is demonstrated in this paper. This preliminary data indicates that flexible 3D CNTs cuff electrode provides an excellent platform for functional electrical stimulation.

**Keywords** Cuff electrode · Carbon nanotubes · Parylene · Peripheral nerve interface

## 1 Introduction

Peripheral nerve stimulation (PNS) has been widely used in medical care, including the treatment of chronic pain (Mironer et al. 2011), restoration of motor functions (Ethier et al. 2012) and etc. Depending on whether electrodes penetrate the nerve fascicles or not, peripheral nerve electrodes are typically divided into extrafascicular electrodes or intrafascicular electrodes (Navarro et al. 2005). Intrafascicular electrodes can achieve high selectivity by placing the electrodes within the fascicles of the nerve. However, nerve damage and long-term stability are concerns. On the other hand, extrafascicular electrode like a

cuff electrode has attracted a lot of attention due to its noninvasiveness and low threshold level (Yu et al. 2014). The cuff electrodes are made by the thin film deposition (Kang et al. 2015). Several electrode modification techniques have been performed to enhance performances. For example, electrode surfaces can be roughened in order to enlarge surface areas (Weremfo et al. 2015). Materials with higher charge capacity are also coated on electrode surfaces, including active carbon (Zhi et al. 2014), iridium oxide (IrOx) (Slavcheva et al. 2004), and poly(3,4-ethylenedioxythiophene) (PEDOT) (Castagnola et al. 2015) and etc. The peripheral nerves are 3-dimensional structures, where individual fiber is connected and motor and sensory information is transmitted. Cuff electrodes are positioned outside the epineurium, and it is challenging to achieve selectivity. Usually, multiple electrode sites are used to enhance the selectivity of cuff electrode (David-Pur et al. 2013). Recently, a polyimide split-ring shaped cuff electrode was designed with four triangular bendable platinum electrodes around the polyimide frame (Lee et al. 2017), where the protruding electrode can be in tight contact with the nerve.

Carbon nanotubes (CNTs) have aroused tremendous interests as implantable electrodes because of their extraordinary electrical and mechanical properties, especially their intrinsically large surface areas (Yi et al. 2015). CNTs are usually synthesized at high temperature, and there have been several studies to coat CNTs to polymer substrates, including layer-

---

Jie Hu and Mark Ming-Cheng Cheng's groups contribute the work equally, and they are listed as co-corresponding authors.

---

✉ Jie Hu  
hujie@sjtu.edu.cn

✉ Mark Ming-Cheng Cheng  
mcheng@wayne.edu

<sup>1</sup> State Key Laboratory of Mechanical System and Vibration, Shanghai Jiao Tong University, Shanghai, China

<sup>2</sup> Electrical and Computer Engineering, Wayne State University, Detroit, MI, USA

<sup>3</sup> Department of Biomedical Engineering, Wayne State University, Detroit, MI, USA

by-layer self-assembly (Zhang et al. 2013), electrodeposition (Keefe et al. 2008), stamping (Kim et al. 2012) and etc. These methods produced a thin 2D mesh-like structure, which may not be as effective as a 3D structure when interfacing with tissues. In our previous study (Yi et al. 2015), the process to integrate on a flexible and biocompatible substrate (parlylene) has been demonstrated. In this paper, we investigated the performance of high-aspect ratio CNTs as cuff electrodes for PNS. Our design may offer many advantages. First, CNTs have large surface areas and a large charge capacity, which can reduce threshold voltage required for nerve activation in PNS. Second, the high-aspect ratio CNT electrode provides better contact by filling the gap that exists between the cuff electrode and nerve. The strong stiffness affords the CNT arrays with resistance to bending and makes it possible for CNTs to penetrate through the epineurium. Finally, the CNTs and flexible parlylene substrate are integrated through a novel sandwich manner to enhance the adhesion, making the device potentially suitable for chronic applications.

## 2 Materials and methods

### 2.1 Device design

The layout of the CNTs cuff electrode is shown in Fig. 1a. The device consists of three parts: CNT microelectrode sites, metal leads, and contact pads for external connection. The overall dimension of the cuff electrode was determined by the targeted peripheral nerve. In this paper, the device was designed to wrap around the sciatic nerve of rats (0.8~1 mm). Figure 1b shows the dimensions of electrode sites and spacing. The electrode sites were composed of vertically grown CNTs. The area of CNT electrode was  $2500 \mu\text{m}^2$ . Two Pt electrodes with area of  $40,000 \mu\text{m}^2$  were also included (labeled as 8 and 16 in Fig. 1b). The spacing of electrodes was chosen to evenly locate around the nerve when the flexible device was wrapped around the rat sciatic nerve. Two holes at the edge of flexible device were used for stitching in order to tie the device onto the nerve (Fig. 1c).

### 2.2 Device fabrication

The fabrication procedures are presented in Fig. 2. First, low stress silicon-rich nitride was grown on a silicon substrate using low pressure chemical vapor deposition (LPCVD) as shown in Fig. 2a. Then 20 nm titanium (Ti) and 200 nm platinum (Pt) were thermally evaporated and patterned by lift-off to serve as electrodes (Fig. 2b). Arrays of holes were defined at the same time to serve as etching windows for the final release step (Fig. 2c). In a second lift-off step, 100 nm titanium nitride (TiN) was selectively patterned on the electrode sites, followed by deposition of a 2 nm iron (Fe) using radio-

frequency sputtering. The wafers were then loaded in a thermal furnace for the CNT growth (Fig. 2d). The growth took place in a gas mixture of ethylene and ammonium ( $\text{C}_2\text{H}_4/\text{NH}_3$ ) at 80 Torr for 120 min. To protect the synthesized CNT arrays from the following process steps, a layer of photoresist was spun to coat the CNTs. Afterwards, a 3  $\mu\text{m}$  thick parlylene C layer was deposited by CVD (Fig. 2e). Then oxygen plasma etching was applied to open the etching holes. Gas-phase xenon difluoride ( $\text{XeF}_2$ ) etchant was applied to remove bulk silicon in the handle wafer (Fig. 2f). This process was simple and CMOS compatible. Subsequently, a second parlylene layer (10  $\mu\text{m}$ ) was deposited to encapsulate the device and seal the etching windows (Fig. 2g). Finally, electrodes and contact pads were opened by oxygen plasma before mechanically releasing the flexible device from the substrate (Fig. 2h and i).

### 2.3 Electrophysiological experiments

The flexible CNT cuff electrode was tested in-vivo. All the procedures in electrophysiological experiments were approved by the Institution Animal Care and Use Committee (IACUC) at Wayne State University. The experiments were performed on the adult male Sprague-Dawley rats weighing 350-400 g. They were sedated and anesthetized by an intramuscular injection of ketamine hydrochloride (43 mg/kg), xylazine (7 mg/kg), and butorphanol (0.1 mg/kg). Supplemental doses of ketamine were administered when prolonged surgery or the animal required to maintain anesthesia. A physiological solution was applied to prevent dry eyes. Skin incision was made in the middle of the thigh, and the inferior gluteal muscle and biceps femoris were blunt dissected to expose sciatic nerve 1 cm in length. After exposing the sciatic nerve, flexible CNTs cuff electrode was wrapped around the nerve. And the cuff electrode was fixed by stitching the two holes on the electrode panel. A pool was formed from skin flaps, and the sciatic nerve was immersed in warm (37 °C) mineral oil to prevent it from drying. The Achilles tendon was separated from the calcaneus together with a small piece of bone, which was clamped by an alligator clamp attached to a load cell (Model SML 10, Interface Inc) to record muscle contraction force. Figure 3 shows the experimental setup for physiological tests. The flexible CNTs cuff electrode was attached to sciatic nerve for stimulation. A rigid CNT electrode was placed on the top of the gastrocnemius to record EMG signals. The signals were amplified, digitized and analyzed using PC-based spike discrimination and frequency analysis software. All software was part of the Computerscope Enhanced Graphics Acquisition and Analysis (EGAA) system (R.C. Electronics, Goleta, CA). The data were also simultaneously recorded on an analog tape recorder (MR-30, TEAC, Montebello, CA).

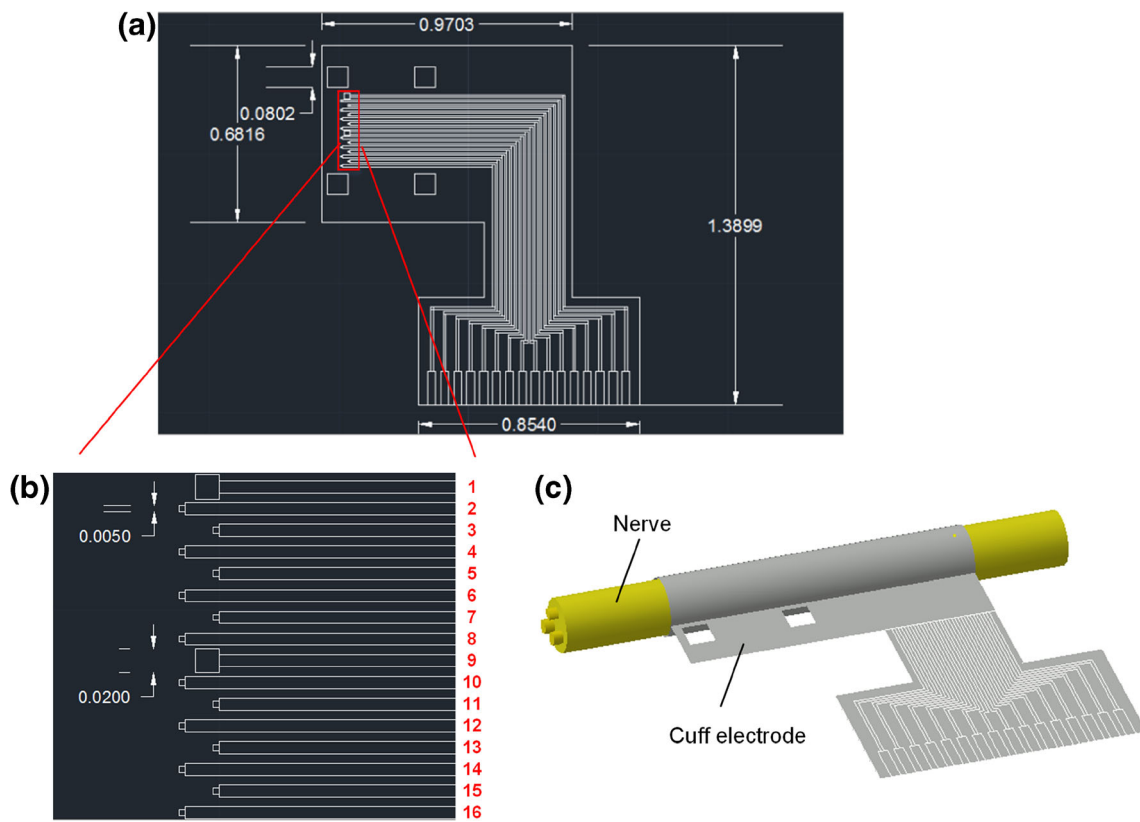


**Fig. 1** **a** The design figure with dimensions of the CNTs cuff electrode (the unit is cm); **b** The magnified figure to show the dimension and spacing of electrode sites; **c** The schematic view when the flexible cuff electrode is wrapped around the nerve

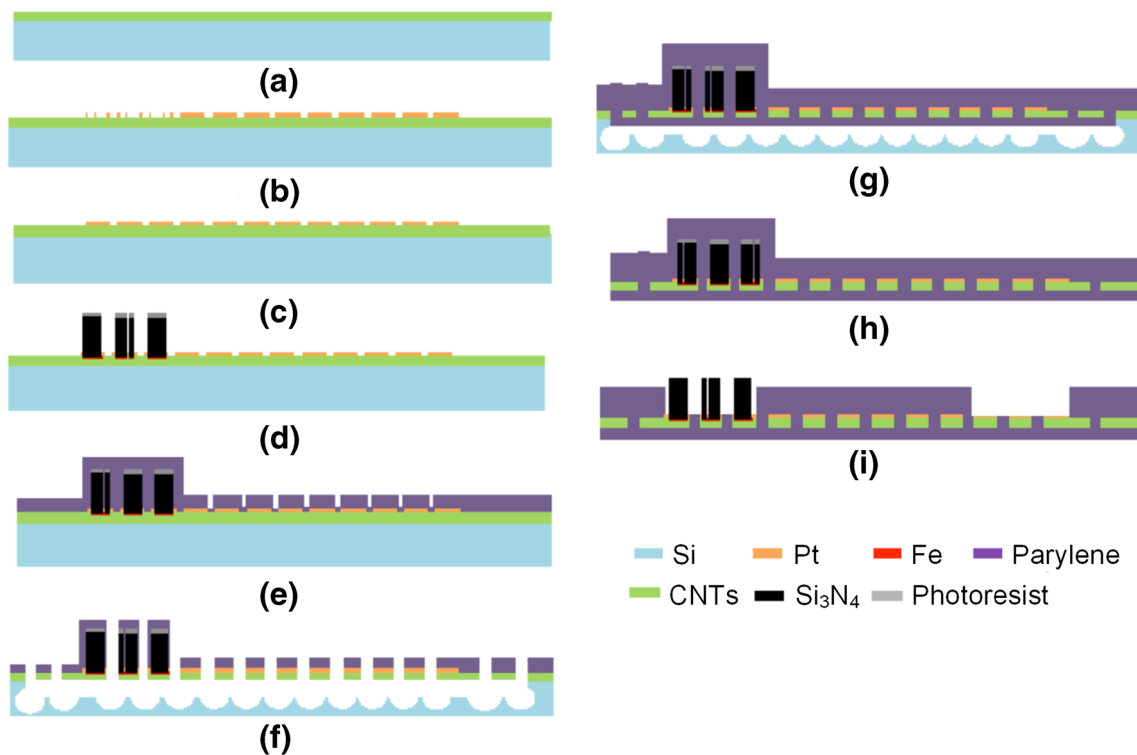
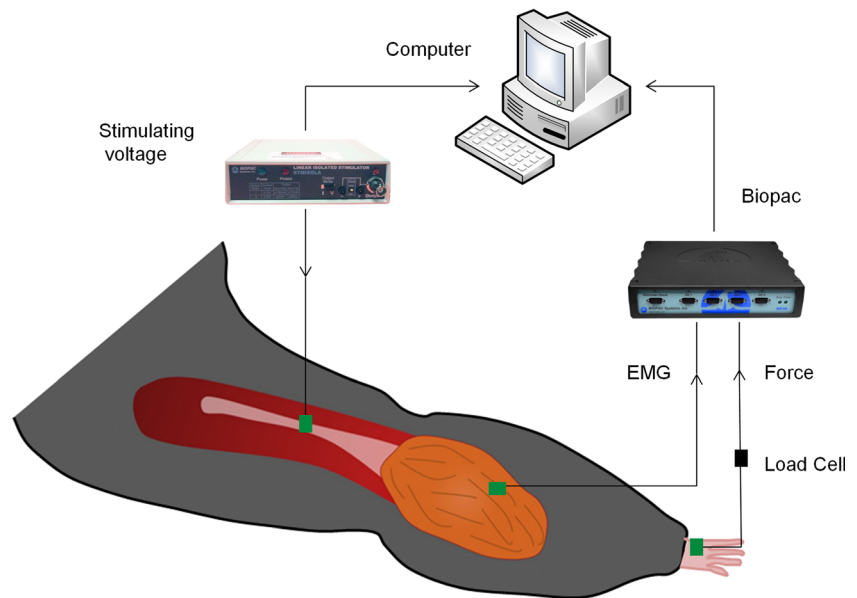


**Fig. 2** Fabrication process of CNTs cuff Electrodes

**Fig. 3** Schematic of experimental setup for physiological tests



### 3 Results and discussion

#### 3.1 Characterization of the device

The image of scanning electron microscopy (SEM) in Fig. 4a presents the morphologies of CNTs grown on a Si substrate before the coating of parylene. The CNTs are well aligned with 60  $\mu\text{m}$  height. The SEM image with lower magnification in Fig. 4b shows the CNTs on the flexible parylene substrate. CNTs are freely standing on the surface, demonstrating the good adhesion between 3D CNTs and parylene. The photograph of the cuff electrode is shown in Fig. 4c. The flexible parylene substrate enables CNTs to be in contacted with PNS and biomedical implants. Figure 4d shows CNTs cuff electrode implanted around the sciatic nerve. The flexible parylene substrate shows good conformity wrapping around the nerve. The electrical connection was done by a flexible printed circuit (FPC). Through this connector, the flexible nerve cuff electrode was connected with electronic instrumentation.

One of the considerations for the design of cuff electrodes is mechanically flexibility. In this work, parylene was chosen as the substrate material for the highly flexible and reformed nerve cuff electrodes. Parylene has been applied in a variety of biomedical devices due to its superior mechanical strength and biocompatibility (Hassler et al. 2010; Xie et al. 2014). A robust parylene substrate also demonstrates a high level of conformability for implantation. In the following, additional factors in design of cuff electrodes are listed for safe and effective electrical stimulation.

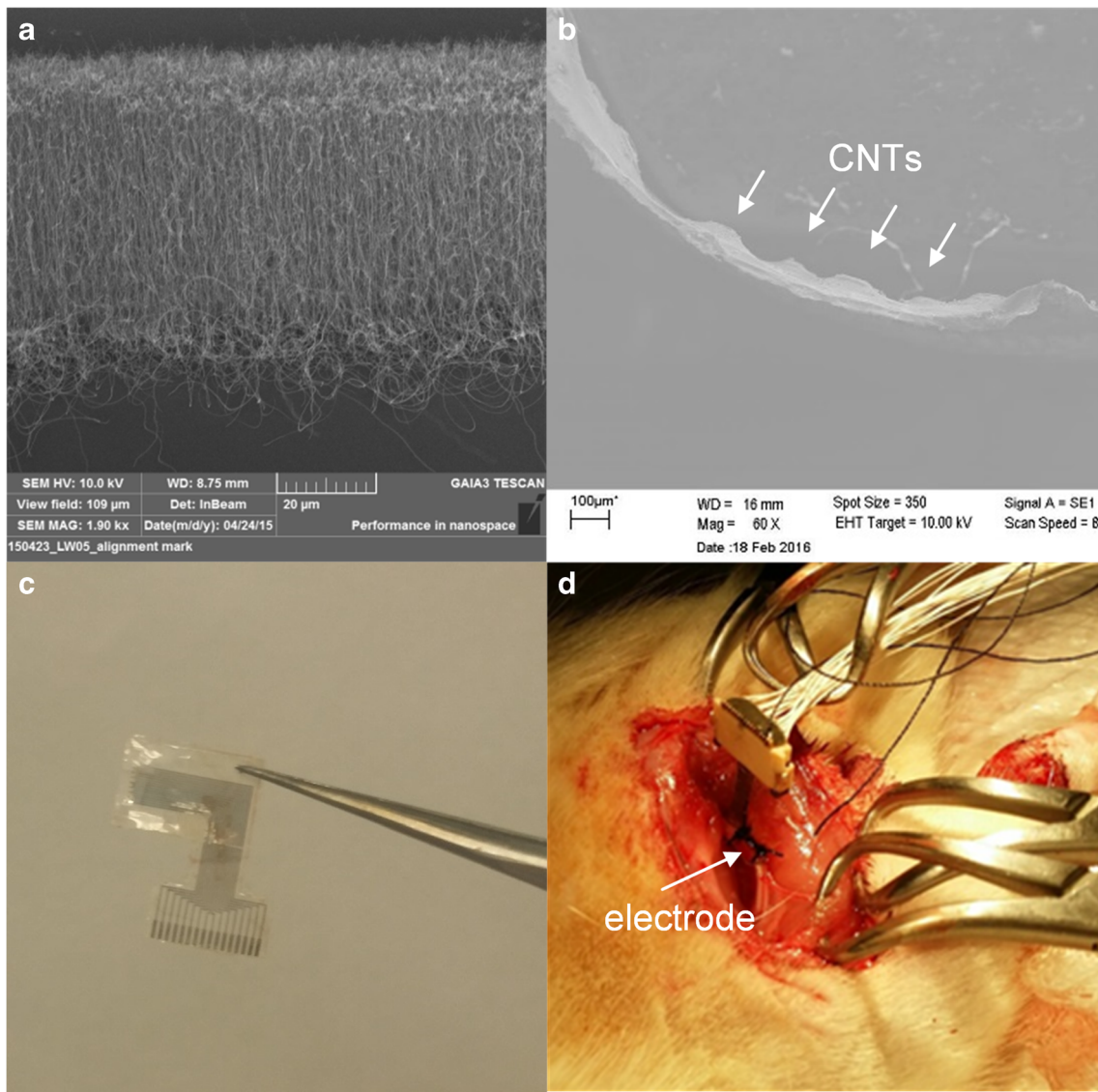
- (1) For safety, the applied stimulation should remain below the charge-carrying capacity of the electrode to avoid irreversible reactions such as water hydrolysis, electrode

dissolution and evolution of gases (Cogan 2008). The electrode material can be engineered to increase active surface areas to support large current injection. Therefore, the stimulus magnitude required for nerve activation could be minimized. In our work, CNTs has been adopted as electrode materials due to its excellent electrochemical properties and large intrinsic surface areas.

- (2) The methods to selectively stimulate different sub-populations of axons are important. In this work, an array of multiple electrode sites has been integrated into the flexible substrate to improve selectivity. The rigid and small-radius of the CNT is more advantageous than normally used planar electrodes. The small dimension of CNTs may cause less tissue damages and it provides better contact with adjacent axons.
- (3) For chronic applications, nerve electrodes have to be stable in a physiologic environment. Poor adhesion between electrode contact and substrate presents one of the most common reasons for electrode failure (Ochoa et al. 2013). The deposition of two-layers of parylene enhances the adhesion between CNTs and the polymer substrate.

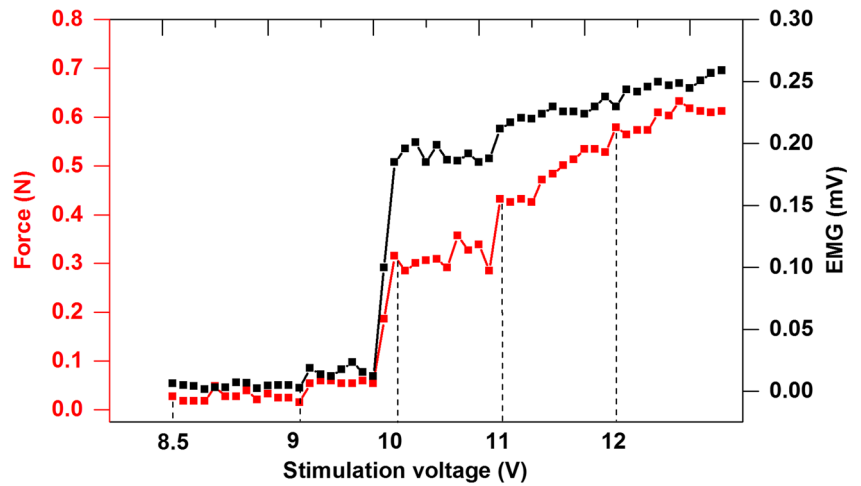
#### 3.2 The performance of CNTs cuff electrode for stimulation

The stimulation voltage was applied in the sciatic nerve by the two different sites of CNTs cuff electrodes. The stimulus was applied to achieve muscle contraction to perform the desired movements. Figure 5 shows the measured the responses of EMG signals and contraction forces generated by the sciatic nerve stimulation. The higher stimulus pulse voltage produced the larger EMG signals and the bigger muscle contraction



**Fig. 4** **a** The synthesized CNTs on a rigid Si substrate; **b** CNTs electrodes integrated on a flexible polymer substrate; **c** The fabricated CNTs cuff electrode; **d** The device implanted around the sciatic nerve

**Fig. 5** The correlation between EMG response and contraction force generated by the sciatic nerve stimulation. The electrode sites were 8 (Pt) and 15 (CNT) with a distance of 0.130 cm





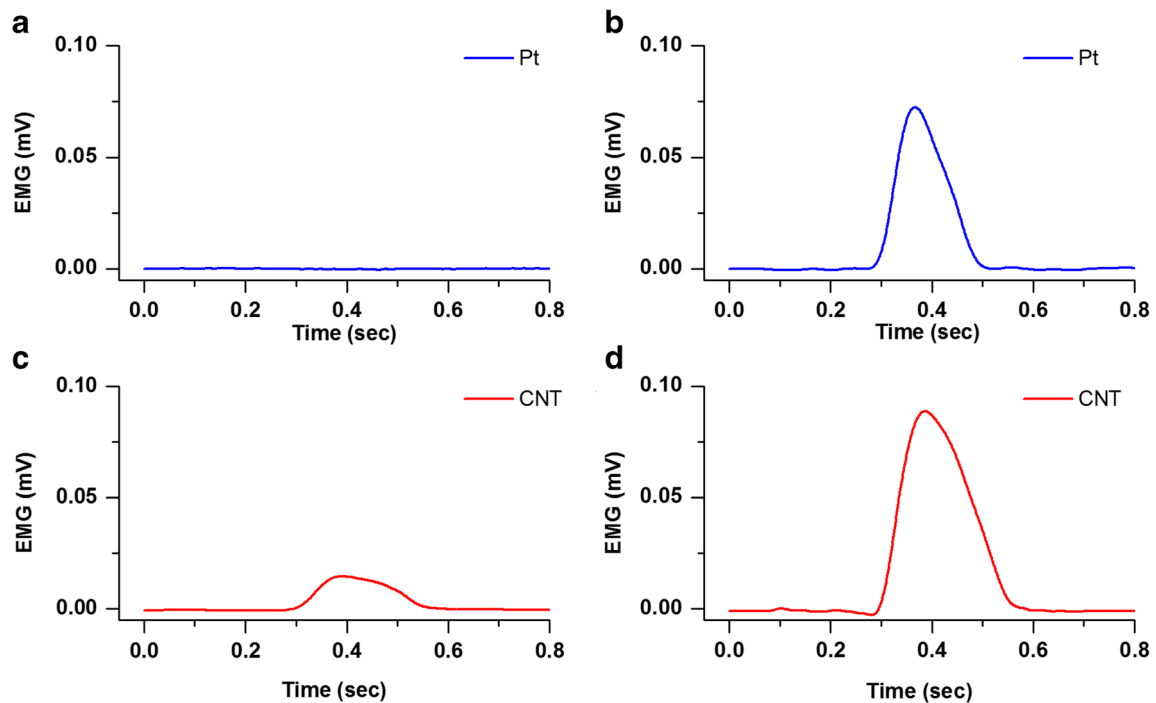


**Fig. 6** In-vivo EMG recording in rats. **a** EMG signals stimulated by Pt electrode at 5.5 V; **b** EMG signals stimulated by Pt electrode at 10 V; **c** EMG signals stimulated by CNT electrode at 5.5 V; **d** EMG signals stimulated by CNT electrode at 10 V

force (Linear correlation, Pearson test,  $p < 0.05$ ). The contraction force generated by the stimulus needs to be properly regulated to reduce the possibilities for muscle damage or fail of function (for example, too much force for grasping will break the target item). This work provides a reliable way to make guidelines for safe functional electrical stimulation for motor function restoration and rehabilitation.

An ideal electrode should have a high charge storage capability (CSC) so that the electrode will not be damaged at high injection current. Our previous study demonstrated that CNT

has a typical CSC of  $30 \text{ mC/cm}^2$ , which was about 6 times larger than that of Pt electrodes. The performance of CNT and Pt as cuff electrode was compared in this study. Figure 6 shows EMG signals stimulated by CNT/CNT and Pt/Pt electrode couples at the same distance. At 5.5 V stimulation, no obvious compound muscle action potential (CMAP) was activated by Pt electrodes (Fig. 6a). While the EMG signals stimulated by CNT electrode exhibited a clear CMAP (Fig. 6c). Figure 6b and d depicts the EMG signals at 10 V stimulation. The duration time and area under curve (AUC) of EMG peak for CNT electrode were larger than Pt electrode (t-test,  $p < 0.05$ ). More axons were excited by CNTs electrodes. The experimental results demonstrated that CNT electrodes could be more effective without creating high voltages that might damage the surrounding tissues. This advantage can be ascribed to enlarged surface area of CNTs.

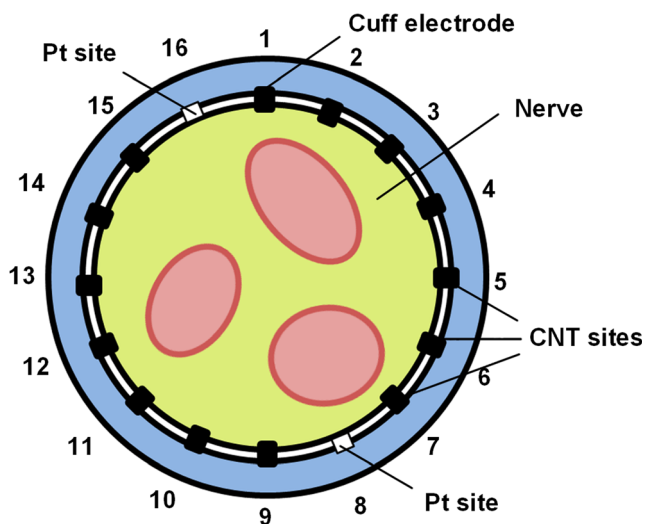


**Fig. 7** The CNTs cuff electrode around the nerve

**Table 1** Five couples of electrodes with different spacing

Group	anode	cathode	Distance
1	8(Pt)	15 (CNT)	0.130 cm
2	8 (Pt)	2 (CNT)	0.106 cm
3	8 (Pt)	13 (CNT)	0.0946 cm
4	8 (Pt)	10 (CNT)	0.0363 cm
5	8 (Pt)	7 (CNT)	0.0263 cm

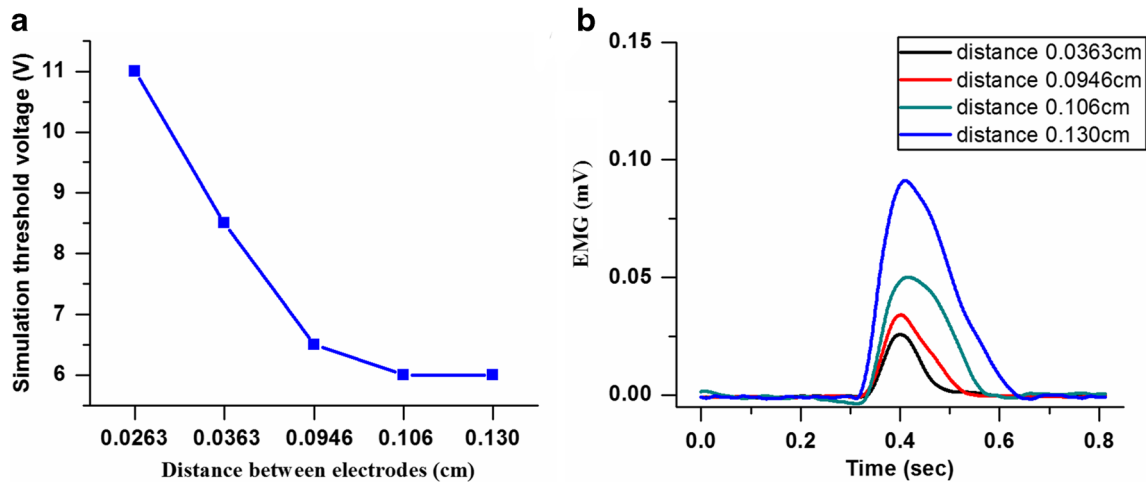


**Fig. 8** a Threshold voltage of 10 V stimulation via electrode pairs positioned at different distances; b EMG signals stimulated by 10 V voltage at different distances

### 3.2.1 Effects of electrode positions

Theoretically, the excitatory field within a cuff electrode could be controlled depending on the distance and stimulation. Hence, it is possible to manipulate the current flow and regulate the particular neural elements to be activated or blocked. In this work, all the 16 electrode sites on a cuff electrode are labeled as shown in Fig. 7 Selective stimulation of the sciatic nerve was performed while CMAPs of the gastrocnemius were recorded to characterize the relationship between muscle activation and stimulation location. Five couples of electrodes with different spacing were chosen as anode and cathode for stimulation as shown in Table 1. To compare the effect of the stimulation position around the nerve epineurium, the threshold voltages of muscle fibers to be excited were recorded at different distances. As shown in Fig. 8a, the electrode couples that positioned further apart will start twitching at lower voltage. It is because that short circuit is formed easily by putting electrodes closely. As a result, the current would mostly flow

through the epineurium. In contrast, current was forced to flow through axons when electrodes were placed far away. Figure 8b shows the EMG signals stimulated by 10 V voltage at different distances. The longer distance between cathode and anode produced the larger duration and higher amplitude of CMAP. Figure 9 shows the AUC and duration of EMG peaks by 10 V stimulation via electrodes at different distances. When electrodes were placed further away, the electrical route was longer, and the number of nerve fiber to be stimulated was bigger. Consequently, the duration and AUC of the EMG peaks was longer for the more separated electrodes.

### 3.2.2 Effect of stimulation frequency

Neural stimulation is a function of the amplitude and frequency of the stimulus pulse. Stimulation frequency determines the output force and the type of contractions thanks to a process known as “sum of contractions” which occurs in the myofibrils. If the muscle fibers are already in a contracted state and

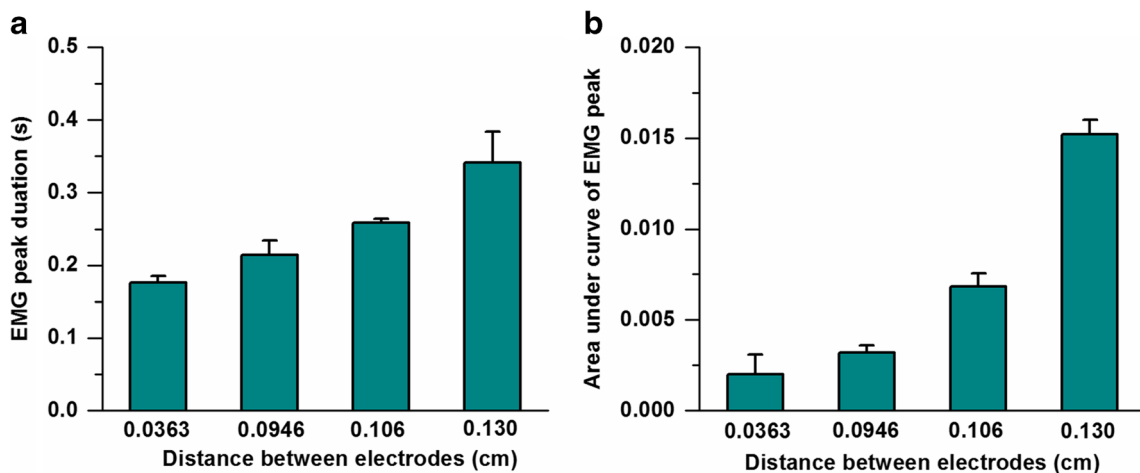


**Fig. 9** a Duration of EMG peaks generated by 10 V stimulation; b AUC of EMG peaks generated by 10 V stimulation

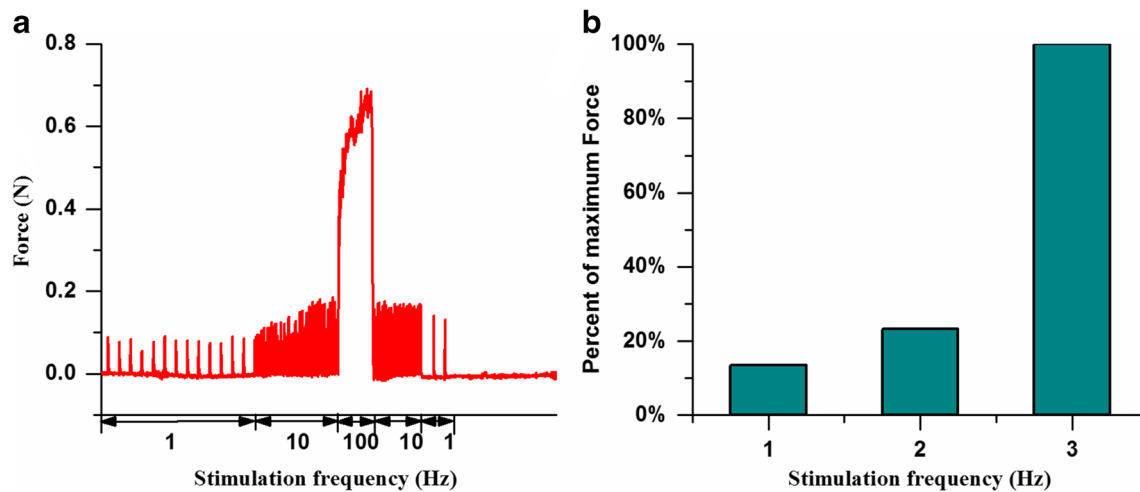


**Fig. 10** **a** EMG magnitude at different stimulation frequency; **b** The percentage of force generated at 1 Hz and 10 Hz related to the normalized force at 100 Hz

not relaxed before another excitatory stimulus is received, an increased force is generated. At low firing frequency, muscle fibers are contracted with small tension and have enough time to relax before next stimulus takes place. At higher firing rate, muscle contracts with higher force magnitude and less distinction of individual twitches. As the frequency keeps increasing and finally exceeds the frequency of tetany, force saturation is achieved. Tetany is the state at which the stimulated muscle will no longer have tremor. As a result, muscle fatigue is inflicted. Figure 10 shows how the muscles responded to different stimulation pulse frequencies (1 Hz, 10 Hz, 100 Hz). At 1 Hz, the muscle fibers had enough time to relax and did not produce any visible muscle tetany. At 100 Hz, the muscle fibers reached the tetany state and the contraction force showed no fluctuation. Our device afforded a good platform to investigate the fatigue effect of muscles.

## 4 Conclusion

A novel flexible multi-site CNT cuff electrode has been demonstrated in this paper. It consists of two layer of parylene which sandwiches not only the conductive CNT electrode and metal trace, but also the SiN as a buffering layer. The protruding CNT electrodes fill the gap that normally exists between the cuff electrode and nerve. This design takes the form of penetrating electrodes to increase the selectivity while using the soft polymer substrate to reduce the invasiveness and minimize the nerve damage. This preliminary data indicates that Flexible 3D CNTs cuff electrode provides an excellent platform for functional electrical stimulation.

**Acknowledgements** The device was fabricated using Nano Fabrication Core (nFab) at Wayne State University. This work was supported by National Science Foundation (NSF) CAREER Award (1055932), NSF

MRI Award (1229635), National Natural Science Foundation of China (51775332, 51675329), Major Project of National Social Science Fund (17ZDA020), Shanghai Committee of Science and Technology (15142200800, 16441906000, 16XD1425000), National Key R&D Program of China (2016YFF0101602, 2016YFC0104104), the State Key Laboratory of Mechanical System and Vibration (MSV201601).

## References

- V. Castagnola, E. Descamps, A. Lecestre, L. Dahan, J. Remaud, L.G. Nowak, C. Bergaud, *Biosens. Bioelectron.* **67**, 450–457 (2015)
- S.F. Cogan, *Annu. Rev. Biomed. Eng.* **10**, 275–309 (2008)
- M. David-Pur, L. Bareket-Keren, G. Beit-Yaakov, D. Raz-Prag, D. Rand, Y. Hanein, *Sensors* **2013**, 1–4 (2013)
- C. Ethier, E.R. Oby, M. Bauman, L.E. Miller, *Nature* **485**, 368–371 (2012)
- C. Hassler, R.P. von Metzner, P. Ruther, T. Stieglitz, *J Biomed Mater Res B Appl Biomater* **93**, 266–274 (2010)
- X. Kang, J.-Q. Liu, H. Tian, B. Yang, Y. Nuli, C. Yang, *J. Microelectromech. Syst.* **24**, 319–332 (2015)
- E.W. Keefer, B.R. Botterman, M.I. Romero, A.F. Rossi, G.W. Gross, *Nat. Nanotechnol.* **3**, 434–439 (2008)
- D.-H. Kim, R. Ghaffari, N. Lu, J.A. Rogers, *Annu. Rev. Biomed. Eng.* **14**, 113–128 (2012)
- S. Lee, S. Sheshadri, Z. Xiang, I. Delgado-Martinez, N. Xue, T. Sun, N.V. Thakor, S.-C. Yen, C. Lee, *Sensors Actuators B Chem.* **242**, 1165–1170 (2017)
- Y.E. Mironer, J.K. Hutcheson, J.R. Satterthwaite, P.C. LaTourette, *Neuromodulation: Technology at the Neural Interface* **14**, 151–155 (2011)
- X. Navarro, T.B. Krueger, N. Lago, S. Micera, T. Stieglitz, P. Dario, *J. Peripher. Nerv. Syst.* **10**, 229–258 (2005)
- M. Ochoa, P. Wei, A.J. Wolley, K.J. Otto, B. Ziaie, *Biomed. Microdevices* **15**, 437–443 (2013)
- E. Slavcheva, R. Vitushinsky, W. Mokwa, U. Schnakenberg, *J. Electrochem. Soc.* **151**, E226–E237 (2004)
- A. Weremfo, P. Carter, D.B. Hibbert, C. Zhao, *Langmuir* **31**, 2593–2599 (2015)
- X. Xie, L. Rieth, L. Williams, S. Negi, R. Bhandari, R. Caldwell, R. Sharma, P. Tathireddy, F. Solzbacher, *J. Neural Eng.* **11**, 026016 (2014)



- W. Yi, C. Chen, Z. Feng, Y. Xu, C. Zhou, N. Masurkar, J. Cavanaugh, M.M.-C. Cheng, *Nanotechnology* **26**, 125301 (2015)
- H. Yu, W. Xiong, H. Zhang, W. Wang, Z. Li, *J. Microelectromech. Syst.* **23**, 1025–1035 (2014)
- H. Zhang, P.R. Patel, Z. Xie, S.D. Swanson, X. Wang, N.A. Kotov, *ACS Nano* **7**, 7619–7629 (2013)
- M. Zhi, F. Yang, F. Meng, M. Li, A. Manivannan, N. Wu, *ACS Sustain. Chem. Eng.* **2**, 1592–1598 (2014)